

LOW-ENERGY SINGLET SECTOR IN THE SPIN-1/2 J_1-J_2 HEISENBERG MODEL ON A SQUARE LATTICE

A. Yu. Aktersky^{a*}, *A. V. Syromyatnikov*^{a,b**}

^a National Research Center “Kurchatov Institute”, Konstantinov Petersburg Nuclear Physics Institute
188300, Gatchina, Leningrad Region, Russia

^b St. Petersburg State University
199034, St. Petersburg, Russia

Received August 4, 2016

Based on a special variant of the plaquette expansion, an operator is constructed whose eigenvalues give the low-energy singlet spectrum of a spin-1/2 Heisenberg antiferromagnet on a square lattice with nearest-neighbor and frustrating next-nearest-neighbor exchange couplings J_1 and J_2 . It is well known that a nonmagnetic phase arises in this model for $0.4 \lesssim J_2/J_1 \lesssim 0.6$, sandwiched by two Néel ordered phases. In agreement with previous results, we observe a first-order quantum phase transition (QPT) at $J_2 \approx 0.64J_1$ from the nonmagnetic phase to the Néel one. A large gap ($\gtrsim 0.4J_1$) is found in the singlet spectrum for $J_2 < 0.64J_1$, which excludes a gapless spin-liquid state for $0.4 \lesssim J_2/J_1 \lesssim 0.6$ and the deconfined quantum criticality scenario for the QPT to another Néel phase. We observe a first-order QPT at $J_2 \approx 0.55J_1$, presumably between two nonmagnetic phases.

DOI: 10.7868/S0044451016120000

1. INTRODUCTION

Frustrated quantum antiferromagnets have provided a convenient playground for the investigation of novel types of many-body phenomena including quantum spin-liquid and nematic phases, novel universality classes of phase transitions, and order-by-disorder phenomena, to mention just a few. One of the canonical models in this field is the spin- $\frac{1}{2}$ Heisenberg antiferromagnet (AF) on a square lattice with nearest-neighbor and frustrating next-nearest-neighbor AF exchange couplings J_1 and J_2 (the J_1-J_2 model), whose Hamiltonian has the form

$$\mathcal{H} = \sum_{\langle i,j \rangle} \mathbf{S}_i \mathbf{S}_j + J_2 \sum_{\langle\langle i,j \rangle\rangle} \mathbf{S}_i \mathbf{S}_j, \quad (1)$$

where we put $J_1 = 1$. Despite the great interest in this model during the last quarter of a century, its properties remain a puzzle in the most frustrated regime with $0.4 \lesssim J_2 \lesssim 0.6$.

This problem has been attacked using many powerful numerical and analytic methods, including variational Monte Carlo (VMC) calculations [1, 2], the density matrix renormalization group (DMRG) method [3, 4], the coupled cluster method (CCM) [5, 6], plaquette [7, 8] and dimer [9–11] series expansions, the tensor network state approach [12, 13], an exact diagonalization [14–16], spin-wave analysis [17], the large- N expansion [18, 19], the hierarchical mean-field approach [20], the bond operator approach [21–23], the functional renormalization group [24], and some others. It is generally believed that Néel ordered phases with the respective AF vectors (π, π) and $(0, \pi)$ (or $(\pi, 0)$) arise at $J_2 \lesssim 0.4$ and $J_2 \gtrsim 0.6$. The properties of the magnetically disordered phase in the intermediate region $0.4 \lesssim J_2 \lesssim 0.6$ are still being actively debated. Among definite conclusions about the nature of this phase are a columnar dimer state [7, 19] and gapped [3] and gapless [1] spin liquids. However, considerable amount of works report plaquette valence bond solid (VBS) states [4, 13, 16, 20, 23] or a sufficiently close proximity of the system to such states [8, 15].

Quantum phase transitions (QPTs) from the paramagnetic phase to Néel ones are of particular interest. A first-order QPT is what we can expect at $J_2 \approx 0.6$ in the Landau–Wilson paradigm of phase transitions due to different broken symmetries in two phases that cannot be connected by a group–subgroup relation.

* E-mail: aktersky@gmail.com

** E-mail: asyromyatnikov@yandex.ru

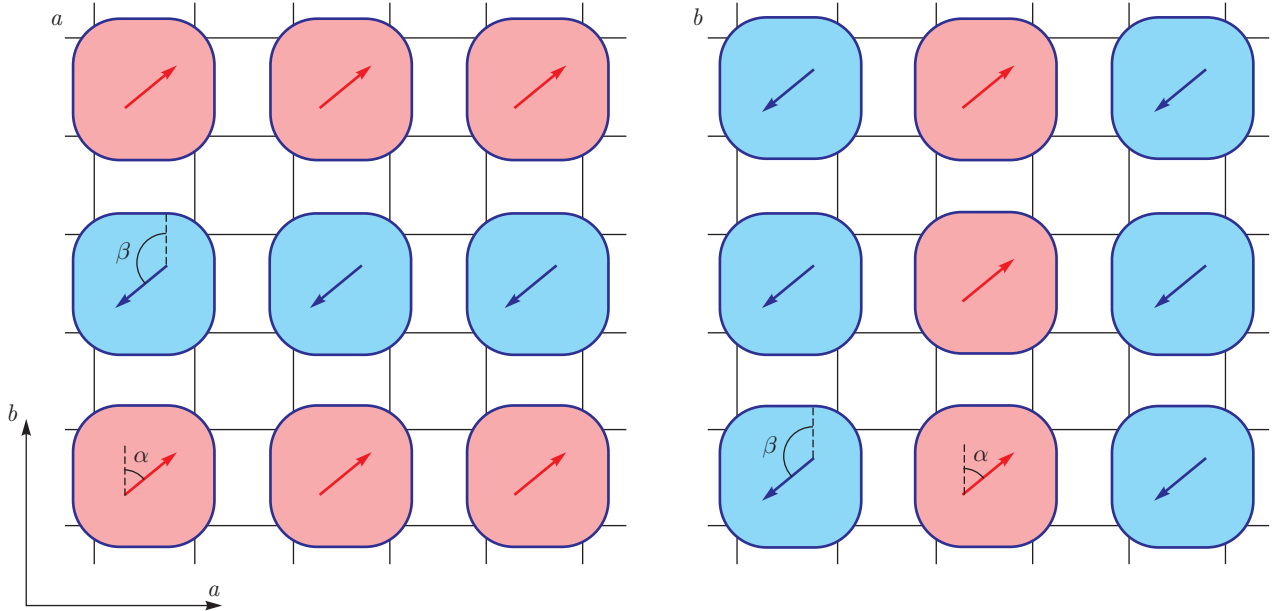


Fig. 1. Sketch of the wave functions of the degenerate ground state with a columnar plaquette structure proposed in this paper at $0.55 < J_2 < 0.64$. Singlet states of each plaquette are described in terms of states of pseudospin-1/2. The orientation of pseudospins in the xz plane of the pseudospin space is depicted by arrows (dashed lines denote the orientation of the z axis in the pseudospin space)

In agreement with this expectation, the majority of works report a first-order QPT at $J_2 \approx 0.6$ (see, e.g., Refs. [3, 4, 7, 10, 12, 13, 20]).

By contrast, the QPT at $J_2 \sim 0.4$ remains a subject of controversy. Within the Landau–Wilson paradigm, one expects a first-order QPT if the C_4 lattice rotational symmetry is broken in the paramagnetic phase [20] (e.g., in the case of a columnar VBS)¹⁾. But it is suggested in Refs. [25, 26] that a second-order QPT can occur in this case via a mechanism of deconfined quantum criticality. Series expansion calculations of magnetic susceptibilities over different perturbation fields suggest a first-order QPT [11], while calculation of the same susceptibilities by the CCM shows a second-order QPT [5]. Recent numerical works obtain an intrinsic structure of the nonmagnetic phase: a disordered phase with gapless triplet excitations at $0.4 \lesssim J_2 \lesssim 0.5$ (Refs. [2, 4, 6]) and a (plaquette [4]) VBS phase with gapped triplet excitations at $0.5 \lesssim J_2 \lesssim 0.6$ (Refs. [2, 4, 12]). Although authors do not exclude the deconfined criticality scenario at a single point or in a wide critical region around $J_2 \sim 0.5$ (quite definite conclusion about its existence can be found in Ref. [12]),

some of them point out that the system size available now for numerical computation is insufficient to make a definite conclusion about the nature of the QPT (see, e.g., the discussion in Refs. [2, 4]).

Using an approach suggested in our previous paper [27], which describes the low-energy singlet sector of model (1)²⁾, we demonstrate below that a first-order QPT arises at $J_2 \approx 0.55$ presumably from the plaquette VBS phase to the plaquette phase having a columnar structure (see Fig. 1). We find that the ground state is separated by a large gap $\gtrsim 0.4$ from the first excited singlet level at $J_2 < 0.64$. Then critical fluctuations cannot arise in the singlet sector, which excludes the deconfined criticality scenario of the QPT to the Néel phase. A gapless spin-liquid state is also inconsistent with this finding. In accordance with previous results, we observe a first-order QPT at $J_2 \approx 0.64$ to another Néel phase. The ground state energies that we obtain for $0.4 \lesssim J_2 < 0.64$ are in good agreement with the results of previous numerical calculations.

The rest of the paper is organized as follows. We describe our approach in Sec. 2. Ground state properties and singlet excitations are discussed in Sec. 3. A

¹⁾ If the C_4 lattice rotational symmetry is unbroken in the paramagnetic phase, a second-order QPT is expected within the Landau–Wilson paradigm [20].

²⁾ The ground state of model (1) was found to be singlet in previous studies while a rigorous proof (Marshall's theorem [29–31]) of its singlet nature exists only for $J_2 = 0$ and $J_2 \rightarrow \infty$.

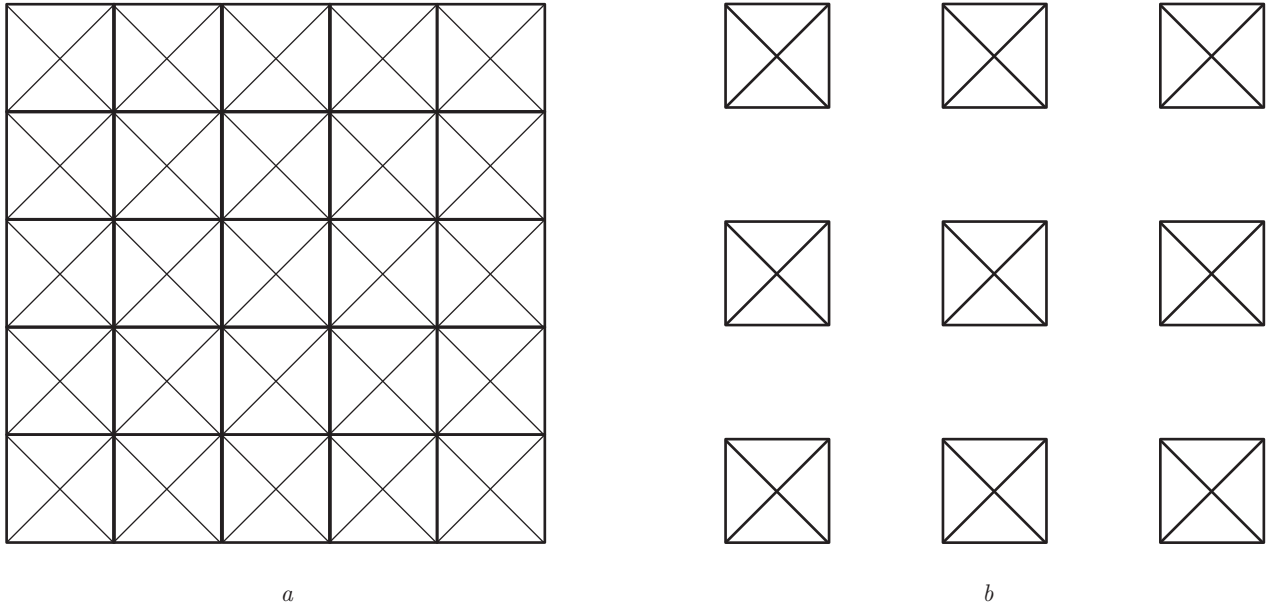


Fig. 2. (a) Model (1) on a simple square lattice and (b) decoupled plaquettes having a doubly degenerate singlet ground state. Bold and thin lines denote exchange interactions with the respective coupling constants $J_1 = 1$ and J_2 . To pass from decoupled plaquettes to model (1), we introduce operator (3) controlled by the parameter λ such that $\lambda = 1$ and $\lambda = 0$ respectively correspond to panels (a) and (b)

summary and conclusions can be found in Sec. 4. An Appendix contains details of the analysis.

2. METHOD AND TECHNIQUE

Because the method we use is discussed in detail in our previous paper [27] devoted solely to singlet excitations at $J_2 = 0$, we describe it only briefly here. We perform a sort of plaquette expansion to derive an operator H (an “effective Hamiltonian”) whose eigenvalues give energies of low-lying singlet levels of model (1). Our starting point is a set of isolated plaquettes in which exchange coupling constants between all four spins are equal to unity (see Fig. 2b). The wave functions of the doubly degenerate singlet ground state of an isolated plaquette

$$\Psi^+ = \frac{\phi_1 + \phi_2}{\sqrt{3}}, \quad \Psi^- = \phi_1 - \phi_2 \quad (2)$$

are constructed as linear combinations of nonorthogonal ones, $\phi_1 = (|\uparrow\rangle_1 |\downarrow\rangle_2 - |\downarrow\rangle_1 |\uparrow\rangle_2)(|\uparrow\rangle_3 |\downarrow\rangle_4 - |\downarrow\rangle_3 |\uparrow\rangle_4)/2$ and $\phi_2 = (|\uparrow\rangle_2 |\downarrow\rangle_3 - |\downarrow\rangle_2 |\uparrow\rangle_3)(|\uparrow\rangle_4 |\downarrow\rangle_1 - |\downarrow\rangle_4 |\uparrow\rangle_1)/2$, which are depicted in Fig. 3. It is convenient to regard Ψ^+ and Ψ^- as states of pseudospin $s = 1/2$, respectively corresponding to $s_z = 1/2$ and $s_z = -1/2$.

To pass from decoupled plaquettes to model (1), we introduce an operator controlled by a single parameter

λ (at a given J_2) that describes interactions between spins from different plaquettes and which weakens interactions between diagonal spins in each plaquette,

$$\begin{aligned} V = & \lambda \left(\sum_{\langle i,j \rangle} \left(\mathbf{S}_2^{(i)} \mathbf{S}_1^{(j)} + \mathbf{S}_3^{(i)} \mathbf{S}_4^{(j)} + \right. \right. \\ & \left. \left. + J_2 \left(\mathbf{S}_2^{(i)} \mathbf{S}_4^{(j)} + \mathbf{S}_3^{(i)} \mathbf{S}_1^{(j)} \right) \right) + \right. \\ & \left. + \sum_{\langle i,p \rangle} \left(\mathbf{S}_1^{(i)} \mathbf{S}_4^{(p)} + \mathbf{S}_2^{(i)} \mathbf{S}_3^{(p)} + J_2 \left(\mathbf{S}_1^{(i)} \mathbf{S}_3^{(p)} + \mathbf{S}_2^{(i)} \mathbf{S}_4^{(p)} \right) \right) + \right. \\ & \left. + (J_2 - 1) \sum_i \left(\mathbf{S}_1^{(i)} \mathbf{S}_3^{(i)} + \mathbf{S}_2^{(i)} \mathbf{S}_4^{(i)} \right) \right), \quad (3) \end{aligned}$$

where the respective upper and lower indexes of \mathbf{S} enumerate plaquettes and indicate the spin number in a plaquette (according to Fig. 3), and $\langle i,j \rangle$ and $\langle i,p \rangle$ respectively denote nearest-neighbor plaquettes in horizontal and vertical directions. Decoupled plaquettes correspond to $\lambda = 0$ and model (1) corresponds to $\lambda = 1$.

The singlet ground state is 2^N times degenerate in the system containing N decoupled plaquettes. This degenerate energy level splits into a singlet band (at $N \rightarrow \infty$) as λ increases because V commutes with the total spin operator. Our goal is to describe this

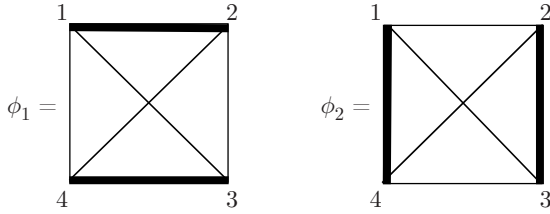


Fig. 3. Wave functions of an isolated plaquette from which its singlet ground-state wave functions (2) are constructed. Bold lines denote singlet states of the corresponding two spins

band in terms of the interaction between pseudospins by performing perturbation calculations up to the 7th order in λ and extrapolating results to $\lambda = 1$ by means of standard methods developed for critical phenomena. We use the standard perturbation theory for systems with degenerate energy levels developed by Bloch and described, e.g., in textbook [28]. Consideration of the corresponding wave functions in the spin space is beyond the scope of this paper. By the symmetry arguments in Ref. [27], it is the low-energy singlet sector of model (1) that we consider in this way: because of the dependence of V on only one control parameter λ and different symmetry properties of Ψ^+ and Ψ^- , no significant overlap is expected of higher-energy singlet bands and the considered one.

3. “EFFECTIVE HAMILTONIAN” ANALYSIS

The part of H containing terms describing interaction between no more than two pseudospins has the form

$$\begin{aligned} H = CN + h \sum_i s_i^z + \sum_{i,j} (J_{ij}^{zz} s_i^z s_j^z + J_{ij}^{+z} s_i^+ s_j^z + \\ + J_{ij}^{-z} s_i^- s_j^z + J_{ij}^{z+} s_i^z s_j^+ + J_{ij}^{z-} s_i^z s_j^- + J_{ij}^{++} s_i^+ s_j^+ + \\ + J_{ij}^{--} s_i^- s_j^- + J_{ij}^{-+} s_i^- s_j^+ + J_{ij}^{+-} s_i^+ s_j^-), \quad (4) \end{aligned}$$

where i and j are not restricted to only nearest-neighbor plaquettes: terms in the perturbation theory of the order higher than three contain two-pseudospin long-range interactions as well as multi-pseudospin interactions. All of them are taken into account in our quantitative consideration below. It should be noted that in accordance with the general property of the perturbation series [28], the operator H is non-Hermitian (e.g., $J^{++} \neq J^{--}$): non-Hermitian terms appear starting from the third order in λ (see Appendix A for the series of some coefficients in H). However, according to the general proof [28], its spectrum must be real. The operator H is translation-invariant: it is defined on the

square lattice whose period is twice as large as the period of the original lattice. We calculate corrections to all parameters in H (including the multi-pseudospin and long-range terms) up to the 7th order in λ . To extrapolate the ground-state energy and the spectrum from $\lambda \ll 1$ to $\lambda = 1$, we use Padé and Padé–Borel resummation techniques. There is no point in applying these techniques individually to each coefficient in H because the number of available terms is small in the series for some of them. Then we derive analytic expressions for physical quantities and find series for them up to the 7th order in λ using series for the coefficients in H .

3.1. Ground state

It is seen from Eq. (4) that H describes an anisotropic magnet in the effective magnetic field h . The magnetic field dominates in H at $\lambda \ll 1$ and $J_2 \lesssim 0.6$ because the first nonzero term in its series is of the first order in λ , whereas the first nonzero terms are of the second order in the series for coefficients of two-pseudospin interaction (see Appendix A for an example). Then, in the first order in λ , the system is equivalent to a set of isolated spins in an external magnetic field with $\langle \mathbf{s}_i \rangle$ directed along the z axis of the pseudospin space. In the second order in λ , a Hermitian two-pseudospin interaction arises in Eq. (4):

$$J_{ij}^{++} = J_{ij}^{--} = J_{ij}^{+-} = J_{ij}^{-+}$$

and

$$J_{ij}^{+z} = J_{ij}^{-z} = J_{ij}^{z+} = J_{ij}^{z-}.$$

As a result, $H = \tilde{H}$ in the second order, where

$$\begin{aligned} \tilde{H} = CN + h \sum_i s_i^z + \sum_{i,j} (J_{ij}^{zz} s_i^z s_j^z + J_{ij}^{xx} s_i^x s_j^x + \\ + J_{ij}^{xz} (s_i^x s_j^z + s_i^z s_j^x)), \quad (5) \end{aligned}$$

where $J_{ij}^{zz}, J_{ij}^{xx} < 0$, and J_{ij}^{xz} have equal moduli and opposite signs on vertical and horizontal bonds (this feature originates from different symmetries of Ψ^+ and Ψ^- : Ψ^+ does not change under plaquette rotation through the angle $\pi/2$, but Ψ^- changes its sign). Consequently, the $\langle \mathbf{s}_i \rangle$ lie in the xz plane of the pseudospin space and, due to inequivalent vertical and horizontal bonds, we have to assume a columnar structure of the ground state shown in Figs. 1a and 1b for $J_{ij}^{xz} > 0$ and $J_{ij}^{xz} < 0$ on vertical bonds. These structures are characterized by two angles α and β determining directions of $\langle \mathbf{s}_i \rangle$ with respect to the z axis. We note that we can obtain both $J_{ij}^{xz} > 0$ and $J_{ij}^{xz} < 0$ on vertical bonds at

a given J_2 using two bases: wave functions are built in the first basis using Ψ^+ and Ψ^- given by Eqs. (2), whereas Ψ^+ and $-\Psi^-$ are used instead in the second basis (i.e., the second basis is obtained from the first by rotation through $\pi/2$). This leads to an additional ground state degeneracy when $\alpha \neq 0$ and/or $\beta \neq 0$. For definiteness, we build bare wave functions using Eqs. (2). As a result of particular calculations, we find that the ground state wave function has the form presented in Fig. 1a in this basis when $\alpha \neq 0$ and $\beta \neq 0$.

At small λ , when the “Zeeman term” dominates in H , $\alpha = \beta = 0$. However, the angles become finite for some J_2 at $\lambda \sim 1$. We find that no improvement is required of the two-angle ansatz after taking other terms in H (including non-Hermitian ones) of higher orders in λ into account. In particular, coefficients in the series for $J_{ij}^{\pm z}$ and $J_{ij}^{z\pm}$ have equal moduli and opposite signs on vertical and horizontal bonds in all orders in λ (see Appendix A for an example).

To obtain a Bose analog of H and find α , β , and the spectrum, it is natural to use the Holstein–Primakoff transformation. We proceed with the non-Hermitian Bose analog of H as with a non-Hermitian Bose analog of a spin Hamiltonian after the Dyson–Maleev transformation in magnetically ordered phases, as this was done in Ref. [27]. To obtain the ground-state energy E_{GS} at a given J_2 , we examine terms in H not containing Bose operators that give a series in λ whose coefficients depend on α and β . Performing the resummation procedure for different values of these angles (spread on a regular grid), we find their values at which the energy is minimal. As in Ref. [27], we also take the first $1/s$ corrections to the ground-state energy into account. While their contribution is quite small, they move E_{GS} closer to the previous numerical results.

At $0 \leq J_2 < 0.55$, the absolute minimum of the energy is located at $\alpha = \beta = 0$, and hence the ground state is nondegenerate in the effective model. The obtained values of E_{GS} are presented in Fig. 4 and Table 1. It is seen that our results are in good agreement with previous numerical findings at $0.2 < J_2 < 0.55$. Quite expectedly, our approach significantly underestimates the ground-state energy deep in the Néel phase at $J_2 < 0.2$ ³⁾. Two equivalent local minima (at $\alpha \approx -2.2$, $\beta \approx 0.8$ and $\alpha \approx 0.8$, $\beta \approx -2.2$) arise at $J_2 \approx 0.5$. Unlike the minimum at $\alpha = \beta = 0$, whose energy increases as J_2 increases, the energy of these lo-

³⁾ A second-order phase transition occurs on the way from $\lambda = 0$ to $\lambda = 1$ to magnetically ordered phase at $J_2 \lesssim 0.4$, which leads to bad convergence of the dimer and plaquette expansions at $\lambda \sim 1$ (see a discussion in Ref. [27]).

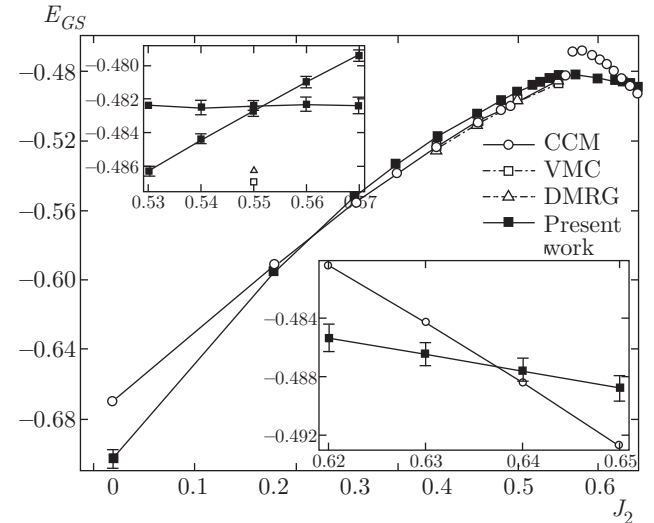


Fig. 4. Ground-state energy per spin E_{GS} obtained using different approaches: the coupled cluster method (CCM) [5, 6], a variational Monte Carlo (VMC) calculation with additional Lanczos improvement steps [1], the density matrix renormalization group (DMRG) method [4], and the plaquette expansion carried out in this paper. See also Table 1 for particular values of E_{GS} . The insets illustrate first-order transitions at $J_2 \approx 0.55$ and $J_2 \approx 0.64$ as a result of the corresponding level crossing

cal minima is almost independent of J_2 . At $J_2 \approx 0.55$, the energy of the minimum at $\alpha = \beta = 0$ becomes equal to that of the two equivalent minima signifying a first-order phase transition (see the upper inset in Fig. 4)⁴⁾. The energy landscape at $J_2 = 0.55$ is presented in Fig. 5⁵⁾. It is seen that all minima are very shallow and the barriers between them are low⁶⁾. This signifies that there are many low-energy states in the system with nearly equal energies at $J_2 \sim 0.5$.

⁴⁾ In particular, at $J_2 = 0.55$, we find the following series for the energy at $\alpha = \beta = 0$ and $\alpha \approx 0.8$ and $\beta \approx -2.2$: $-0.375 - 0.05625\lambda - 0.0530599\lambda^2 + 0.00645224\lambda^3 - 0.00679466\lambda^4 + 0.00411219\lambda^5 - 0.00415998\lambda^6 + 0.00778856\lambda^7$ and $-0.375 + 0.0304735\lambda - 0.0952434\lambda^2 - 0.0203372\lambda^3 - 0.00943256\lambda^4 - 0.00518608\lambda^5 - 0.00292147\lambda^6 - 0.00853038\lambda^7$, respectively. These series give as the result of the resummation procedure $-0.4827(3)$ and $-0.4824(3)$.

⁵⁾ Interestingly, we can obtain a picture similar to Fig. 5 in model (5), e.g., at $|J^{xz}| \sim |J^{xx}| \sim |J^{zz}|$ with negative J^{xx} and J^{zz} and an appropriate h value. Our analysis of the series for these three coefficients J shows that these relations between them are likely to be valid. Then the reduced variant of “effective Hamiltonian” (5) gives qualitatively correct results.

⁶⁾ The convergence of series is much better near minima than in the region between them: the estimated error near all minima is $3 \cdot 10^{-4}\mathcal{N}$ (\mathcal{N} is the number of spins in the system) while it is an order of magnitude larger between the minima. We can then only roughly estimate the barrier height between minima as $0.004(2)\mathcal{N}$.

Table 1. Values of the ground-state energy per spin for some J_2 , which are also shown in Fig. 4. Note that VMC and DMRG data for $J_2 = 0.4, 0.45$ are available for finite systems only. The procedure of extrapolation to the thermodynamical limit is expected to give slightly higher energies [1, 4]

J_2	Plaquette expansion	VMC ^a	DMRG	CCM ^c
0.4	-0.5180(3)	-0.52333	-0.5253 ^b	-0.52354(4)
0.45	-0.5042(3)	-0.5094	-0.5110 ^b	-0.50964(12)
0.5	-0.4924(3)	-0.49717	-0.4968 ^c	-0.4984(2)
0.55	-0.4827(3)	-0.48698	-0.4863 ^c	-

^a Ground-state energies per spin in $L \times L$ systems with $L = 18$. ^b Ground-state energies per spin in systems with $L = 10$.

^c Values extrapolated to the thermodynamic limit $L \rightarrow \infty$.

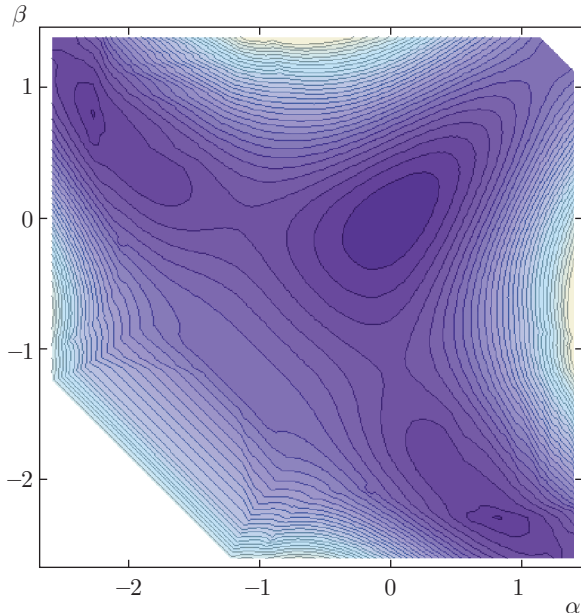


Fig. 5. Ground-state energy per spin as a function of angles α and β at $J_2 = 0.55$ near local minima. Contours connect points with the same energy and points in darker regions have lower energies. The energy difference between points on neighboring contours is $0.0011\mathcal{N}$, where \mathcal{N} is the number of spins in system (1). The minimum at $\alpha = \beta = 0$ and two equivalent minima at $\alpha \approx -2.2, \beta \approx 0.8$ and $\alpha \approx 0.8, \beta \approx -2.2$ have approximately the same energy

Because we do not examine ground-state wave functions in the spin space in this paper, it is difficult to say definitely what phases correspond to the energy minima at $J_2 \approx 0.55$. It seems unlikely, however, that the minimum at $\alpha = \beta = 0$ corresponds to the Néel phase at $J_2 \approx 0.55$ because the majority of previous considerations report the Néel phase stability at $J_2 < 0.4 \div 0.5$ (the widest range, $J_2 < 0.532$, of the Néel phase stabil-

ity is obtained in Ref. [12]). Bearing in mind that the majority of previous studies report the plaquette VBS phase at $J_2 > 0.5$, it looks reasonable to suppose that the minimum at $\alpha = \beta = 0$ corresponds (at $J_2 \approx 0.55$) to the plaquette VBS state, while a columnar plaquette VBS phase (with an additional two-fold degeneracy of the ground state) corresponds to two equivalent minima (see Fig. 1). However, further consideration is needed to determine the properties of these two phases precisely. Because we do not obtain the singlet gap closure at $J_2 < 0.64$ (see below), a transition to the Néel phase is expected upon the triplet gap closure at $J_2 < 0.55$ (the Néel phase would also correspond to the minimum at $\alpha = \beta = 0$).

At $J_2 > 0.55$, another local minimum arises at $\alpha, \beta \sim 4$, which definitely becomes the absolute minimum at $J_2 = J_{c2} > 0.6$, signifying another first-order QPT. However the convergence of the series at that region of the phase space is very bad (presumably because the decoupled plaquettes are too bad a starting point for the description of the Néel phase at $J_2 > 0.6$). Then, for an accurate determination of J_{c2} , we have to compare the energy of the local minimum at $\alpha \approx 0.8, \beta \approx -2.2$ with the energy of the Néel phase found before numerically using another approach (we choose data from Refs. [5, 6] obtained by the coupled cluster method). As is seen from the lower inset in Fig. 4, the first-order transition occurs at $J_2 \approx 0.64$, in agreement with many previous results (see, e.g., Refs. [3, 4, 7, 10, 12, 13, 20]).

3.2. Singlet excitations

The spectrum of singlet excitations is found by the analysis of the terms in H bilinear in Bose operators, as is done in Ref. [27]. The singlet spectra at $J_2 = 0.55$ are shown in Fig. 6 corresponding to minima at $\alpha = \beta = 0$

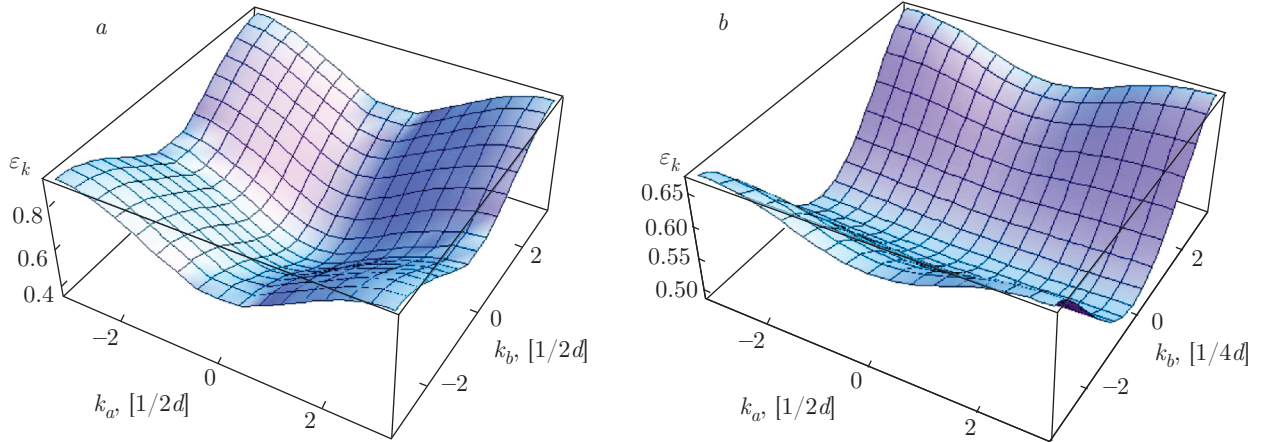


Fig. 6. Spectra of singlet excitations ϵ_k at $J_2 = 0.55$ corresponding to (a) ground state energy minimum at $\alpha = \beta = 0$ and (b) that at $\alpha \approx 0.8$, $\beta \approx -2.2$ (see Fig. 5). Here d is the distance between nearest-neighbor spins in model (1) and $k_{a,b}$ are components of \mathbf{k} in the coordinate system shown in Fig. 1a

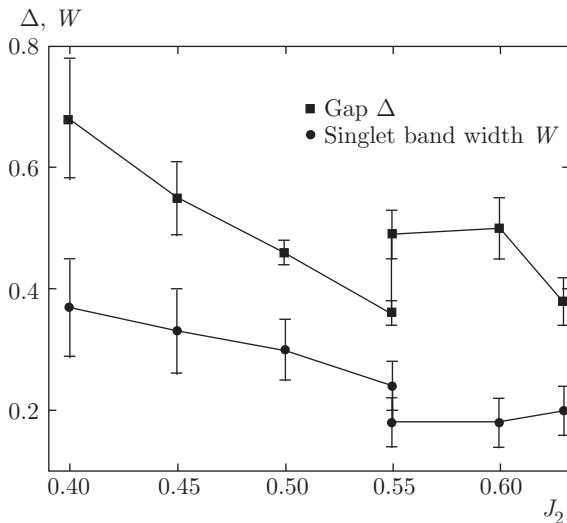


Fig. 7. Gap Δ in the singlet spectrum and the low-energy singlet band width W

and at $\alpha \approx 0.8$, $\beta \approx -2.2$. Remarkably, the singlet spectra have quite large gaps at $J_2 < 0.64$, whose values are presented in Fig. 7. At $J_2 < 0.55$, the gap is located at $\mathbf{k} = \mathbf{0}$. The small dispersion of the spectrum along the a axis (see Fig. 1a) at $J_2 > 0.55$ does not allow determining the gap location on the line $(-\pi, 0) - (\pi, 0)$. Estimating the first $1/s$ corrections to the spectrum demonstrates a very small renormalization by quantum fluctuations of pseudospins.

4. CONCLUSION

To conclude, we construct the operator H whose eigenvalues coincide with energies of low-energy singlet states of the spin-1/2 J_1-J_2 Heisenberg model (1) on a

square lattice. Parameters of H are found in the first seven orders of the perturbation theory. Using series for the coefficients, we obtain series for the ground-state energy and the singlet spectrum. It is expected that our approach is particularly suitable for discussing the plaquette phase observed in many previous papers at $0.4 \lesssim J_2 \lesssim 0.6$. After a standard resummation procedure, we obtain the ground-state energies presented in Fig. 4 and Table 1. In accordance with the results of previous considerations, we find a first-order transition from the magnetically disordered phase to the Néel phase at $J_2 \approx 0.64$. We also observe a first-order QPT at $J_2 \approx 0.55$. Bearing in mind the results of previous considerations, it seems unlikely that this QPT separates another Néel phase and the nonmagnetic one (because we analyze only the singlet spectrum in the present study, we cannot make a definite conclusion about the properties of the phases). We suppose that this is a QPT inside the nonmagnetic region between the plaquette phase (stable at $J_2 < 0.55$) and the phase arisen at $0.55 < J_2 < 0.64$, which presumably has the columnar plaquette structure with additional twofold ground state degeneracy related to the rotational symmetry breaking (see Fig. 1). However, further consideration is needed to determine the properties of these two phases precisely.

The singlet spectrum is found to be gapped at $J_2 < 0.64$ (see Fig. 7), which makes either a spin-liquid state in the nonmagnetic region or the deconfined quantum criticality scenario for the transition to the Néel phase at $J_2 < 0.55$ impossible. The latter transition would be characterized by a closure of only the triplet gap.

Table 2. Nonzero coefficients of the “effective Hamiltonian” in the first seven orders in λ describing interaction between nearest and next-nearest neighbor pseudospins at $J_2 = 0.55$. Subscripts h , v , and d denote the shortest horizontal, vertical, and diagonal bonds between pseudospins. The constant C also has a zeroth-order correction equal to $-\lambda^0 3/2$, which is given by the ground-state energy of an isolated plaquette

	1	2	3	4	5	6	7
C	0.225	-0.324427	-0.061202	-0.050632	-0.010787	-0.028230	-0.009198
h	0.9	-0.332917	-0.277432	-0.105482	-0.102216	-0.037882	-0.110016
J_h^{zz}	0	-0.108542	-0.085331	-0.035047	-0.033701	-0.008582	-0.028041
J_h^{--}	0	-0.081406	0.044564	0.042000	0.097999	0.034800	0.146126
J_h^{++}	0	-0.081406	-0.028701	-0.073196	-0.073308	-0.090835	-0.102988
$J_h^{+-} = J_h^{-+}$	0	-0.081406	0.007932	0.000887	0.011299	0.005432	0.017833
$J_h^{-z} = J_h^{z-}$	0	-0.094000	-0.011220	0.051871	0.053753	0.014496	-0.089420
$J_h^{+z} = J_h^{z+}$	0	-0.094000	-0.053520	-0.041564	-0.063113	0.013452	0.076528
J_d^{zz}	0	0	-0.013664	-0.017605	0.004330	-0.001672	0.020554
J_d^{--}	0	0	0.010248	0.009056	0.044433	0.027467	0.041915
J_d^{++}	0	0	0.010248	-0.009390	-0.039010	-0.042935	-0.042100
$J_d^{+-} = J_d^{-+}$	0	0	0.010248	-0.000167	-0.004437	-0.003411	-0.006107
J_v^{zz}	0	-0.108542	-0.085331	-0.035047	-0.033701	-0.008582	-0.028041
J_v^{--}	0	-0.081406	0.044564	0.042000	0.097999	0.034800	0.146126
J_v^{++}	0	-0.081406	-0.028701	-0.073196	-0.073308	-0.090835	-0.102988
$J_v^{+-} = J_v^{-+}$	0	-0.081406	0.007932	0.000887	0.011299	0.005432	0.017833
$J_v^{-z} = J_v^{z-}$	0	0.094000	0.011220	-0.051871	-0.053753	-0.014496	0.089420
$J_v^{+z} = J_v^{z+}$	0	0.094000	0.053520	0.041564	0.063113	-0.013452	-0.076528

We thank J. Richter for the exchange of data. This work is supported by the Russian Science Foundation (grant No. 14-22-00281).

APPENDIX A

Coefficients of the “effective Hamiltonian” at $J_2 = 0.55$

The coefficients of “effective Hamiltonian” (4) are shown in Table 2 in the first seven orders in λ describing interaction between nearest-neighbor and next-nearest-neighbor pseudospins at $J_2 = 0.55$. Numerous coefficients for long-range and multi-pseudospin interactions have also been calculated. They are also taken into account in the quantitative analysis carried out in this paper and can be provided upon request.

REFERENCES

1. W.-J. Hu, F. Becca, A. Parola, and S. Sorella, Phys. Rev. B **88**, 060402 (2013).
2. S. Morita, R. Kaneko, and M. Imada, J. Phys. Soc. Jpn. **84**, 024720 (2015).
3. H.-C. Jiang, H. Yao, and L. Balents, Phys. Rev. B **86**, 024424 (2012).
4. S.-S. Gong, W. Zhu, D. N. Sheng, O. I. Motrunich, and M. P. A. Fisher, Phys. Rev. Lett. **113**, 027201 (2014).
5. R. Darradi, O. Derzhko, R. Zinke, J. Schulenburg, S. E. Krüger, and J. Richter, Phys. Rev. B **78**, 214415 (2008).
6. J. Richter, R. Zinke, and D. J. J. Farnell, Eur. Phys. J. B **88**, 2 (2015).
7. R. R. P. Singh, Z. Weihong, C. J. Hamer, and J. Oitmaa, Phys. Rev. B **60**, 7278 (1999).

8. M. Arlego and W. Brenig, Phys. Rev. B **78**, 224415 (2008).
9. O. P. Sushkov, J. Oitmaa, and Z. Weihong, Phys. Rev. B **66**, 054401 (2002).
10. O. P. Sushkov, J. Oitmaa, and Z. Weihong, Phys. Rev. B **63**, 104420 (2001).
11. J. Sirker, Z. Weihong, O. P. Sushkov, and J. Oitmaa, Phys. Rev. B **73**, 184420 (2006).
12. L. Wang, Z.-C. Gu, F. Verstraete, and X.-G. Wen, arXiv:1112.3331.
13. J.-F. Yu and Y.-J. Kao, Phys. Rev. B **85**, 094407 (2012).
14. J. Richter and J. Schulenburg, Eur. Phys. J. B **73**, 117 (2010).
15. M. Mambrini, A. Läuchli, D. Poilblanc, and F. Mila, Phys. Rev. B **74**, 144422 (2006).
16. L. Capriotti and S. Sorella, Phys. Rev. Lett. **84**, 3173 (2000).
17. P. Chandra and B. Doucot, Phys. Rev. B **38**, 9335 (1988).
18. N. Read and S. Sachdev, Phys. Rev. Lett. **66**, 1773 (1991).
19. N. Read and S. Sachdev, Phys. Rev. Lett. **62**, 1694 (1989).
20. L. Isaev, G. Ortiz, and J. Dukelsky, Phys. Rev. B **79**, 024409 (2009).
21. V. N. Kotov and O. P. Sushkov, Phys. Rev. B **61**, 11820 (2000).
22. R. L. Doretto, Phys. Rev. B **89**, 104415 (2014).
23. M. E. Zhitomirsky and K. Ueda, Phys. Rev. B **54**, 9007 (1996).
24. J. Reuther and P. Wölfle, Phys. Rev. B **81**, 144410 (2010).
25. T. Senthil, A. Vishwanath, L. Balents, S. Sachdev, and M. P. A. Fisher, Science **303**, 1490 (2004).
26. T. Senthil, L. Balents, S. Sachdev, A. Vishwanath, and M. P. A. Fisher, Phys. Rev. B **70**, 144407 (2004).
27. A. Y. Aktersky and A. V. Syromyatnikov, J. Magn. Magn. Mater. **405**, 42 (2016).
28. A. Messiah, *Quantum Mechanics*, Vol. II, North-Holland, Amsterdam (1961).
29. W. Marshall, Proc. R. Soc. London Ser. A **232**, 48 (1955).
30. E. Lieb and D. C. Mattis, J. Math. Phys. **3**, 749 (1962).
31. A. Auerbach, *Interacting Electrons and Quantum Magnetism*, Springer, New York (1994).